

Direct Observation of the Translational Immobilization of Water Molecules Under Nanoscale Confinement

Alec A. Beaton¹ and John M. Franck¹

¹Department of Chemistry, Syracuse University, Syracuse, NY 13210, USA*

(Dated: Tuesday 13th June, 2023 Please note: This is a preliminary version, with subsequent arxiv versions expected.)

Here, Overhauser Dynamic Nuclear Polarization (ODNP) analyzes the translational dynamics of water confined inside reverse micelles (RMs). ODNP offers a unique insight into the translational diffusion of water inside RMs, in particular measuring the diffusion in an “reverse micelle (RM)-fixed” frame (relative to the spin label), rather than relative to the laboratory frame. This study seeks to confirm whether or not the act of tuning the size of the RMs, which can be achieved simply by adjusting the “water loading” (w_0 , *i.e.* the mole ratio of surfactant to water) offer a near-continuous tuning of the translational diffusion of water. The results here confirm this supposition, while offering two additional interesting observations (1) surprisingly, translational diffusion slows to a near-stop for RMs that are small, but that still contain hundreds of water molecules in their core and (2) even relatively large RMs exhibit translational dynamics in their core (center) that is only as fast as translational dynamics on the surface of a lipid bilayer; extrapolation to larger sized water pools implies the need for tens of thousands of water molecules present in a confined pool in order to recover bulk-like translational dynamics. The parts of this study that take place at the lowest water loadings represent the first known instance of an ODNP measurement where the probing spin label interacts continuously with a full complement of water molecules (as opposed to sitting buried inside a lipid membrane or protein core), and yet clearly observes only slow translational diffusion of water. The particular system here, with an NMR-silent CCl_4 dispersant, shoud prove easy to reproduce. Thus, this study also opens up the pathway to future measurements where RMs serve as a ruler for dynamics, in particular for smaller resonance frequencies that can ostensibly detect the dynamics of the slower water inside severely confined (*i.e.* small) RMs.

I. Introduction

RMs are an important model system for understanding confined water, one of only a few systems where size of enclosure can be changed without changing the chemical identity of the enclosing structure [1, 2]. Although applied in the past to study water in materials systems such as Nafion [3] and porous silica preparations [4], ODNP has not yet been used to investigate the water dynamics of RMs. Important work was done in characterizing protein-encapsulated RMs, but the main focus was on using the combination of ODNP and RMs as a vehicle for signal enhancement of the protein Nuclear Magnetic Resonance (NMR) [5]. Toward this end, we have embarked on the first comprehensive measurement of the water dynamics within RMs using ODNP.

Previous measurements using infrared spectroscopy have found that the translational motion decreases as the w_0 decreases and have found difficulty correlating these measurements to the commonly-accepted core/shell model for the water inside these RMs [6, 7]. Other measurements relying on Quasi-Elastic Neutron Scattering (QENS) and molecular dynamics (MD) simulations have found that the translational motion of water is greatly reduced in small RMs [8]. This work is particularly interested in studying the translational motion of water inside Aerosol-OT (AOT) RMs as a function of w_0 to compare these results to those existing in the literature and

to see if any additional insight can be gleaned through these measurements. For these first comprehensive measurements of the internal water pool using ODNP, CCl_4 was elected as dispersant, in order to minimize complications from the dispersant contribution to the signal analysis. In addition to the obvious motivation for simpler signal analysis using ^1H NMR, these results are more directly comparable to QENS [8] and some infrared [6] spectroscopy work which was also conducted in CCl_4 . RMs prepared in dispersants containing protons will subsequently be discussed in a future publication.

To provide appropriate controls, in addition to ODNP measurements, further system characterization was performed by complementary high-field work, invoking both the ^2H screening technique reported in [9] and Paramagnetic Relaxation Enhancement (PRE). PRE is a well-established NMR technique in which the presence of nearby spin probes causes nearby nuclei to relax more rapidly than they would in the absence of the spin probe [10]. In this way, PRE can be used to obtain distance information in, *e.g.* biological systems, where a chemically tethered spin probe (in this case, also known as a spin label) can be used to report on nuclei near that spin label.

II. Theory

The motions observable by ODNP are described by the cross-relaxivity, k_σ , and the slow motional relaxivity, k_{low} . The value of k_{low} can be determined from the cross-

* jmfranck@syr.edu

relaxivity and the self-relaxivity, k_ρ , given by

$$k_{low} = \frac{5}{3}k_\rho - \frac{7}{3}k_\sigma \quad (1)$$

where k_ρ is defined as

$$k_\rho = \frac{((T_{1,p=0})^{-1} - (T_{1,0,p=0})^{-1})}{C_{SL}} \quad (2)$$

where $T_{1(p=0)}$ is the T_1 relaxation time of the sample in consideration with a spin probe concentration of C_{SL} at no microwave power ($p = 0$) and $T_{1,0(p=0)}$ is the T_1 relaxation time of this same sample without any spin probe present.

The cross-relaxivity, k_σ , measures motion on the timescale of the translational motion of water, where as k_{low} measures motion on a slower timescale, such as proton exchange [11, 12].

The unitless parameters $(\frac{k_\sigma}{k_{\sigma,bulk}})^{-1}$ and $(\frac{k_{low}}{k_{low,bulk}})^{-1}$ enable facile comparison to existing ODNP measurements in the literature, as described in [13]. The bulk values of $k_\sigma = 95.4 \text{ M}^{-1}\text{s}^{-1}$ and $k_{low} = 366 \text{ M}^{-1}\text{s}^{-1}$ will subsequently be used to complete this analysis [11].

In addition to ODNP measurements, further system characterization was performed by Electron Spin Resonance (ESR) as well as complementary high-field work, invoking both the ^2H screening technique reported in [9] and PRE. PRE is a well-established NMR technique in which the presence of nearby spin probes causes nearby nuclei to relax more rapidly than they would in the absence of the spin probe [10]. In this way, PRE can be used to obtain distance information in, *e.g.* biological systems, where a chemically tethered spin probe (in this case, also known as as a spin label) can be used to report on nuclei near that spin label.

In some ways PRE can be thought of as a complement to ODNP work, as the samples amenable to ODNP should in principle be amenable to PRE, with the primary reason for this duality owed to the need for a stable unpaired electron present in the system (*i.e.* spin probe). As with ODNP, PRE is brought about by dipolar interaction between an electron spin and a nuclear spin. The dipolar interaction between nuclear spin I and electron spin S in the extreme narrowing limit contributes to T_1 and T_2 relaxation equally as:

$$\frac{1}{T_1} = \frac{1}{T_2} = \frac{\hbar^2 \gamma_I^2 \gamma_S^2}{r^6} \tau_c \quad (3)$$

where γ_I and γ_S are the gyromagnetic ratios of the nuclear spin and electron spin, respectively, r is the distance between the spins, and τ_c the correlation time of the molecule containing the nuclear spin, under the assumption that the electron spin relaxes too quickly to be affected by motion on this timescale [14, 15]. Of note in Eq. (3), however, is the squared dependence on γ_S , which is large relative to the gyromagnetic ratios of nuclear spins such as ^1H and ^2H . As such, dipolar relaxation in the presence of unpaired electrons is the dominant relaxation mechanism in proton NMR, where its

contribution to $1/T_1$ is very large. However, γ_I is $6.5 \times$ smaller for ^2H than it is for ^1H , and as such, this relaxation mechanism contributes negligibly in deuterium NMR [16].

III. Experimental

Two spin probes were studied in this work: TEMPOL (4-hydroxy-2,2,6,6-tetramethylpiperidin-1-oxyl), and the ionic TEMPO- SO_4 (4-sulfate-2,2,6,6-tetramethylpiperidin-1-oxyl potassium salt), as shown in Fig. 1. These nitroxide moiety is located on a neutral molecule in TEMPOL and on a negatively charged ion in TEMPO- SO_4 .

TEMPO- SO_4 was synthesized using the procedure described in Winsberg et al. as it is not commercially available [17]. The lowest and highest w_0 RMs were prepared first, and intermediate w_0 samples were prepared by mixing appropriate aliquots from each in order to keep the concentration of AOT constant across all sample preparations. The constant AOT concentration (as opposed to a constant water concentration) in all samples better suits the ability to background subtract contributions to the NMR signal. The lowest water loading sample ($w_0 = 1$) was prepared by adding AOT (4.37 g, 0.01 mol) to 6.765 mL (10.8 g) CCl_4 . The clear solution was vortexed until all AOT was dissolved, after which 179 μL of 70 mM TEMPO- SO_4 was added to the solution and vortexed 30 seconds 3 \times . The highest water loading sample ($w_0 = 10$) was prepared by adding AOT (4.44 g, 0.01 mol) to 6.765 mL CCl_4 and dissolving completely, after which 1800 μL of 70 mM TEMPO- SO_4 was added to the solution and vortexed for 30 seconds 3 \times . After vortexing, each sample was capped, wrapped in parafilm, placed in a desiccator, and allowed to sit at room temperature for several hours. The final solutions had a slight red color (arising from the nitroxide), more noticeable in the $w_0 = 10$ sample. These preparations correspond to mass percentages of 63, 29, and 11% for the $w_0 = 10$ sample and 70, 29, and 1% for the $w_0 = 1$ sample for CCl_4 , AOT, and water, respectively.

To prepare the $w_0 = 5$ sample, 2070 μL of each the $w_0 = 1$ and $w_0 = 10$ samples were combined to give a final solution volume of 4140 μL . To prepare the $w_0 = 7$ sample, 1320 μL of each the $w_0 = 5$ and $w_0 = 10$ samples were combined to give a final solution volume of 2640 μL . These solutions were vortexed for 30 seconds 3 \times and allowed to become fully transparent before mixing subsequent aliquots or preparing NMR samples. After attaining full transparency, each sample exhibited a slight red color as with the initial $w_0 = 10$ solution.

To prepare the parallel D_2O samples, the same preparation was followed with equivalent amounts of a 70 mM TEMPO- SO_4 D_2O solution used in place of the H_2O solution. The parallel D_2O samples provide background signal to account for any enhancement of the AOT protons that contribute to the detected signal, as in the work by Valentine and coworkers [5].

Given that these samples were prepared in CCl_4 , the

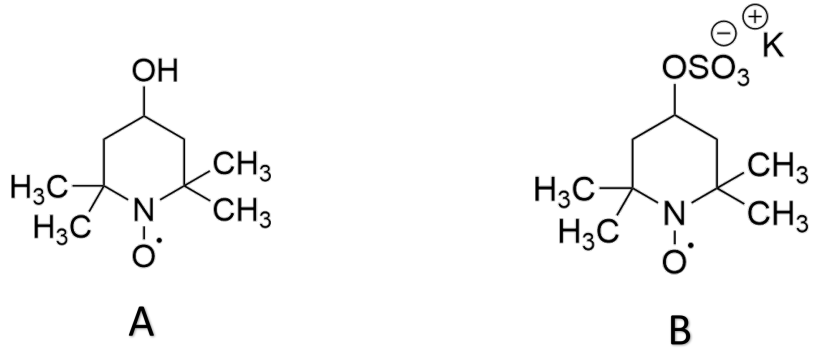


FIG. 1. The spin probes used in this study: (A) TEMPOL and (B) TEMPO-SO₄.

highest w_0 attainable is around 10, thus posing an inherent limitation on the extent to which the RM size can grow [18].

IV. Discussion

IV.1. Spin Probe Localization by PRE

It was previously reported that zwitterionic spin probes have a greater preference for localization inside the internal water pool compared to neutral spin probes [19]. These measurements dealt largely with stearate-derived spin probes which are generally larger than the spin probes studied here (Fig. 1). Toward that end, we sought to explore the localization preferences of TEMPOL and TEMPO-SO₄ in order to determine which, if any, would better suit ODNP experiments (*i.e.* which of the two is more localized to the internal water pool). T₁ measurements were recorded for RM samples containing just water (purple), TEMPOL (blue), and TEMPO-SO₄ (red) for a RM of $w_0 = 8$, shown for the following key regions of the NMR spectra of these chemical systems: around 4 ppm for the water peak (Fig. 2a), around 1 ppm for the aliphatic AOT peak (Fig. 2b), and around 0 ppm for the TMS peak (Fig. 2c). If either spin probe spends any amount of time in the water, near the surfactant, or in the dispersant (as read out from the TMS peak, which is expected to reside in the dispersant), then we should observe a reduced T₁ at these chemical shifts. If there is no reduction in the T₁, then that largely implies the spin probe is kept away from this chemical entity. If the reduction in T₁ is the same for both spin probes, then this implies that each spin probe has approximately equal localization with respect to that chemical entity. If the reduction in T₁ is greater in the presence of one spin probe over the other, however, that indicates that the spin probe producing the greater reduction on T₁ exhibits the greater PRE effect and is more greatly localized by that chemical entity.

In Fig. 2a, both the red and blue contours exhibit a reduced T₁ relative to the control (“empty” water pool) in purple, indicating that there is a PRE taking place in both cases (*i.e.* that both spin probes spend some time

in the water pool). However, the PRE is greater for the red contour, indicating that there is greater localization of TEMPO-SO₄ in the water pool relative to TEMPOL. As observed in Fig. 2a, a PRE effect is again observed in Fig. 2b in the presence of both spin probes, but each spin probe appears to be affecting the same T₁ reduction on the AOT peaks. This indicates that both spin probes have somewhat of a localization near the AOT but that neither spin probe shows a particular preference for the surfactant chains. Lastly, a PRE effect is observed in Fig. 2c for both spin probes, but shown to be greater for the blue contour than the red contour. This indicates that TEMPOL may approach dispersant, where the TMS residues, more frequently relative to the TEMPO-SO₄.

These results support the expectation for greater localization of TEMPO-SO₄ in the internal water pool relative to TEMPOL, with the latter spending more time approaching the dispersant, likely owed to the differences in polarity (charged *vs* not charged) of these two spin probes. Given the interest in studying the water dynamics of the internal water pools, ODNP measurements on RMs containing TEMPO-SO₄ were subsequently performed.

IV.2. Spin Probe Perturbation detected by ²H Relaxometry

Although a sense of the spin probe localization was determined in Sec. IV.1, it is still possible that the presence of the spin probe could potentially perturb the RM system in a manner that is not traceable with the PRE measurements of that section. Toward that end, the Deuterium relaxometry screening technique described in [9] was applied to study the TEMPO-SO₄ loaded RM system. In this way, the spin probe acts like the inclusion molecules studied in [9]. This technique could offer insight into any changes to the hydrogen bonding strength or rotational mobility of water in this RM system. Unlike with ¹H and the work described in the previous section, however, ²H does not exhibit a dramatic PRE effect in the presence of unpaired electrons [16]. As a consequence, the resulting relaxometry data should not reflect much of a change relative to the “empty” RM system.

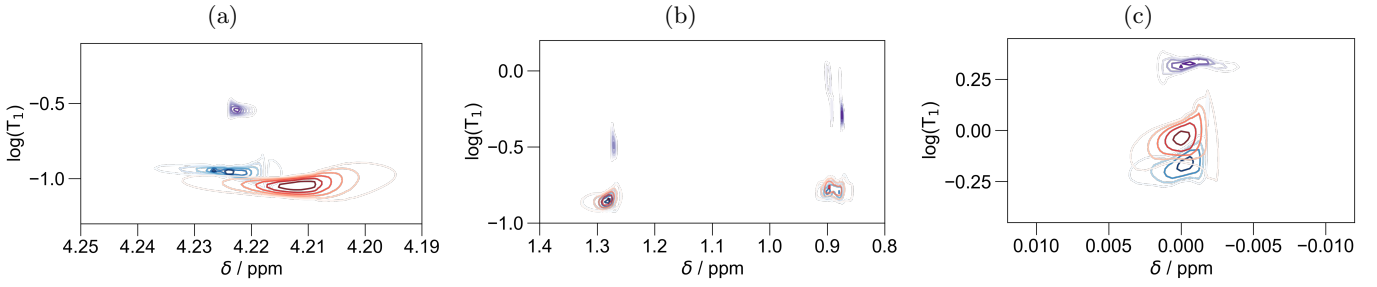


FIG. 2. The water (a) surfactant (b) and TMS (c) regions of the PRE spectra for RM samples prepared with just water (purple), 70 mM TEMPOL (blue), and 70 mM TEMPO-SO₄ (red).

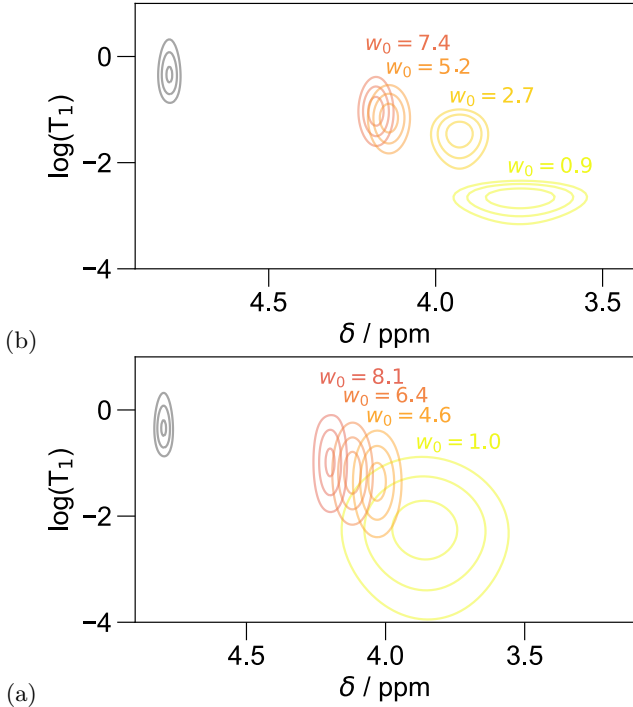


FIG. 3. ILT plot showing the T_1 of D_2O for different AOT RMs prepared in CCl_4 ((a)) and in CCl_4 with added spin probe TEMPO-SO₄ ((b)) for water loadings ranging from 1 to 8.

The results obtained for TEMPO-SO₄ loaded RMs are presented in Fig. 3b, with sample preparations ranging from $w_0 = 1.0$ to 8.1 . The expected behavior is observed – namely, that there is an increase in T_1 and chemical shift as w_0 increases. When compared to the results of Fig. 3a in [9], which correspond to RMs of similar sizes in the same dispersant (CCl_4) but without any spin probe, there is negligible difference apart from potentially wider range of T_1 distributions. This is consistent with the data obtained in the presence of guest molecules present in high concentrations, such as the glucose and PEG-200 data reported in [9]. This indicates that the spin probe does not dramatically perturb the rotational motion or hydrogen bonding network of the internal water pool at the concentration (70 mM) used.

IV.3. Measurements of Translational Diffusivity

IV.3.A. Electron Spin Resonance

Before performing ODNP, the RM samples were analyzed by cw ESR at 9.8 GHz in Fig. 4. In line with previous measurements [19, 20], the ESR spectra show a restriction of the spin probe mobility at the lowest water loadings ($w_0 = 1$, blue) and an incremental increase in the mobility as the w_0 increases, up to the highest w_0 in these measurements ($w_0 = 10$, red). Specifically, the ESR spectra for nitroxide spin probes inside RMs exhibit a characteristic decrease in intensity of the three hyperfine lines from lowest to highest field due to the motional restriction of the spin probe within the confines of the RM. This supports the claim that at all w_0 studied here, RMs were successfully formed. The most upfield hyperfine line is the most sensitive to this motional restriction, as shown in Fig. 4; there is substantial broadening at $w_0=1$ (blue), and it gradually becomes sharper with increasing w_0 (green, orange, and red). This is consistent with the notion that the water pool is developing more bulk-like character with increasing w_0 and that the microviscosity decreases with increasing w_0 . Notably, the spectrum for the highest w_0 studied here ($w_0 = 10$) still does not exhibit hyperfine lines of equal intensity, as expected for a spin probe free in solution, thus indicating that there is still some amount of rotational retardation.

The field concomitant with the lowest field hyperfine line was used as the B_0 field for ODNP measurements. The exact field position was determined before each ODNP experiment by performing a field sweep of the NMR resonance with 3 W of incident microwave power, thus identifying the field position at which maximum enhancement occurs (approximately 3490 G for a microwave frequency of 9.8 GHz).

IV.3.B. Overhauser DNP

With confidence in the spin probe localization within the internal water pool and evidence for this placement not dramatically perturbing the RM water pool properties, along with ESR spectra supporting proper encapsulation of the spin probe itself, ODNP measurements were performed on these RMs. The enhancements for the four different w_0 RMs are shown in Fig. 6 after proper background subtraction of the AOT signal, shown in Fig. 5.

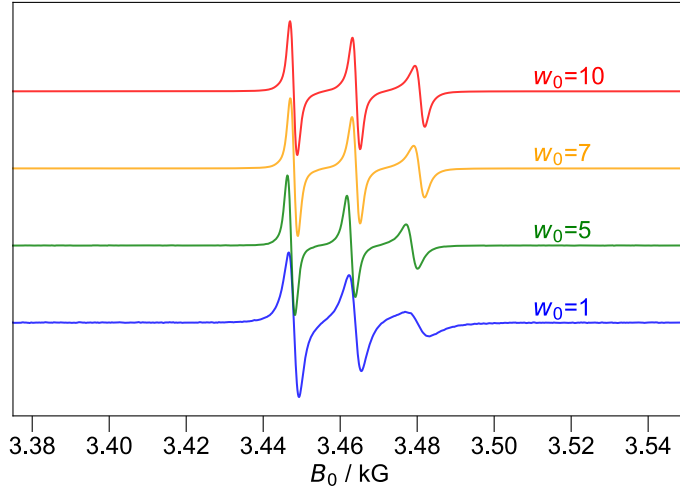


FIG. 4. Normalized ESR spectra acquired for the RM samples containing TEMPO-SO₄ in H₂O for $w_0 = 1$ (blue), 5 (orange), 7.6 (green), and 10 (red).

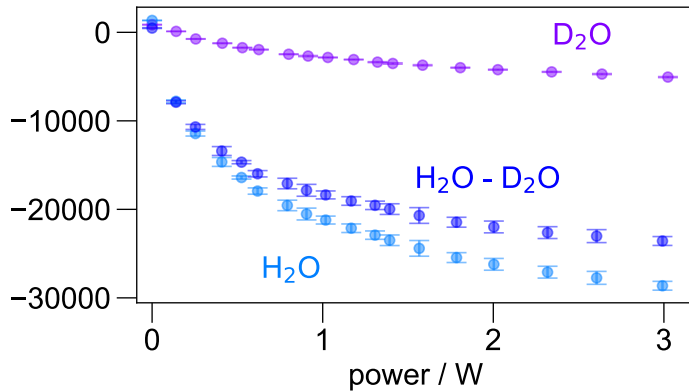


FIG. 5. The unnormalized enhancement curves for $w_0 = 10$ AOT/CCl₄ RMs, showing the difference between a sample prepared with H₂O vs D₂O. The subtraction is performed on the unnormalized data and also shown.

The lowest water loading (blue, $w_0 = 1$) shows very little Overhauser effect in the detected NMR signal, as indicated by the lack of any signal inversion at high powers. Notably, however, the enhancements still follow a clearly asymptotic power dependence and indicate clear saturation of the ESR transition and presence of the ODNP effect. This is consistent with a dramatically motionally restricted water matrix.

The other RMs show increasingly greater enhancement with increasing w_0 , which is also consistent with the increased mobility of the internal water pool detected by ESR. In order to compare this data to other measurements, the cross-relaxivity or k_σ of each sample that shows measurable enhancement is desired.

The fits to the data which produce k_σ are shown in Fig. 7, with the corresponding values tabulated in Table I, which shows an increase in k_σ as the w_0 increases. These values subsequently indicated an expected increase in the mobility of the water in these internal water pools as the RM grows in size. Comparing to the k_σ of bulk water of 95.4 M⁻¹ s¹ [11], these values further indicate

w_0	k_σ (M ⁻¹ s ⁻¹)
1	0.19
5	0.87
7.4	10.6
10	19.1
bulk	95.4

TABLE I. Values for k_σ determined for different RM samples, along with the measurement for bulk water [11].

that at the highest w_0 studied here, the translational motion in the internal water pool is still relatively less than that observed in bulk water close to k_σ of surface of lipid bilayer [13]. These results also indicate that translational mobility is vastly reduced to essentially non-existent in the smallest water pools (w_0 consistent with previous reports from QENS measurements [8]. Taken in a greater context, this supports the concept that translational motion of water is a collective process requiring several water molecules in order for it to take place [21, 22]. At

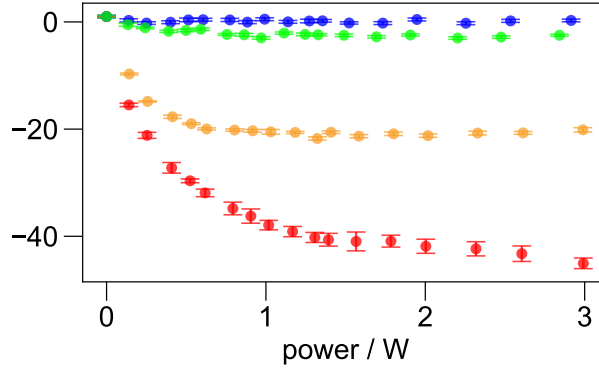


FIG. 6. The enhancement curves for the AOT/CCl₄ RMs for $w_0 = 1$ (blue), 5 (green), 7.4 (orange), and 10 (red). Each has been corrected for the corresponding enhancement of the AOT.

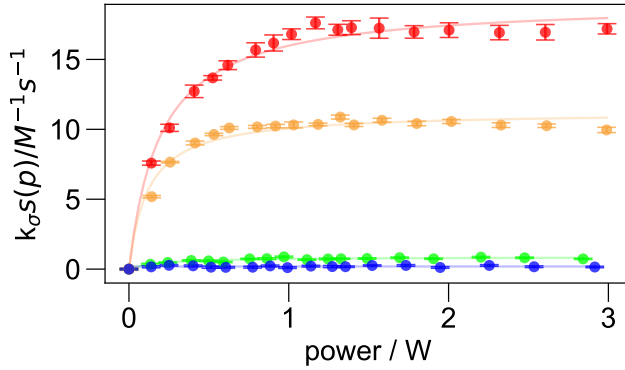


FIG. 7. The results of ODNP measurements are fit to extract k_σ for the two RM systems with observable translational motion, $w_0 = 5$ (green), 7.4 (orange), and 10 (red), with respective values of $0.87 \text{ M}^{-1} \text{ s}^{-1}$, $10.6 \text{ M}^{-1} \text{ s}^{-1}$, and $19.1 \text{ M}^{-1} \text{ s}^{-1}$, indicating a substantial reduction in translational motion.

very small water loadings, the reduced number of water molecules does not provide enough of a water matrix to support translational motion; as the water pool grows in size, more water molecules are present to participate in this water matrix, enabling greater amounts of translational motion.

Lastly, $(\frac{k_\sigma}{k_{\sigma,bulk}})^{-1}$ was determined for each k_σ value reported above, resulting in values of 310, 68, 8.4, and 5.0 for $w_0 = 1, 5, 7.4$, and 10, respectively. The greater this value, the slower the motion of the associated water molecules, which is indicating a gain in water motion as the RM grows. Furthermore, the $(\frac{k_{low}}{k_{low,bulk}})$ values were determined to be .81, .84, .99, and .99, with the latter two points within reasonable amount of error. In comparison to other measurements, these values agree well with values determined for water at the surface of liposomes [12, 13].

Finally, we considered various fits to interpolate and extrapolate the dynamics as a function of w_0 . The simpler option, shown in Fig. 8, involves simply observing that the cross-relaxation, k_σ , hits a baseline at slightly less than $w_0 = 5$, and then fitting the points above this to a straight line. As expected, for the small water pools

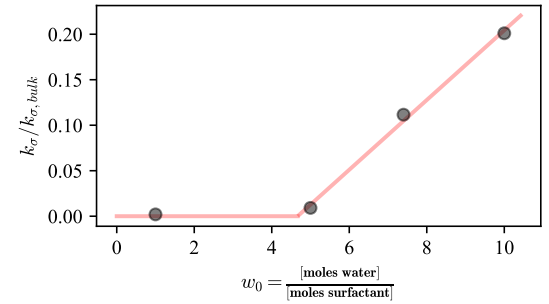


FIG. 8. The determined k_σ values in $\text{M}^{-1} \text{ s}^{-1}$ for each RM measured here plotted against diameter of the water pool in nm, shown in red. A best fit polynomial line in black and extrapolation to the bulk water value near $95.4 \text{ M}^{-1} \text{ s}^{-1}$ is shown in green, at a value of 6.7 nm. If the extrapolation were assumed to be linear, and even greater size RM would be required.

present at low water loadings, the dearth of different hydrogen bonding rearrangements possible leads to a slowdown in the translational motion of the water molecules. However, the lengthscale at which this effects sets in is

surprising: a RM of $w_0 = 4.5 - 8$ encapsulates hundreds of water molecules [7]. Furthermore, extrapolating this straight line to a value of $k_\sigma/k_{\sigma,bulk} = 1$ indicates that the translational dynamics of water could reach bulk-like dynamics at a water loading of $w_0 = 29$; again, the relatively large size of the water pool required proves surprising, as RMs of this lengthscale contains tens of thousands of water molecules. Extrapolating a quadratic fit of the k_σ vs. the water pool diameter indicates a water pool diameter of 6.7 nm is needed which is roughly $w_0 = 20$, although not quite as large, this gain confirms that a very assembly of water molecules is needed to provide bulk-like translational dynamics. This could provide useful insight for future experimentation using ODNP. Ultimately future experimentation is required to better determine the w_0 at which k_σ approaches bulk water. However, it is important to note that the largest sized RM observed here is already accepted to contain thousands of water molecules [7].

V. Conclusion

ODNP provides a localized measurement of water motion by reporting on the motion of water molecules in the vicinity of an electron spin probe. This measurement takes the form of a cross relaxation rate that increases with water mobility. While previous ODNP studies have reported slow water motion at buried sites where rel-

atively few water molecules can access the spin probe, no previous studies have reported very low translational mobility near spin probes that were exposed to significant populations of water molecules. Here, such extreme slow-moving water is achieved at room temperature by confining water inside RMs. Additionally, while other techniques can report on dielectric fluctuations inside RMs, using either bulk- or probe-based methodologies, as well as neutron scattering to report on bulk averaged motion, this is the closest that anyone has come to measuring the translational dynamics of the water in the center of the RM, a fact that is supported with PRE studies of the spin probe location as well as ESR. For the relatively small volumes of water that are possible inside RMs employing the NMR-silent solvent CCl_4 , we observe a near-total shutdown of translational mobility for water pools of diameter ~ 1.75 nm. If the translational mobility and cross-relaxivity follow a linear trend, a diameter of ~ 11 nm ($w_0 \sim 31$) would be required before the water in the center of the pool moved at rates approaching those seen in bulk solution. These measurements provide greater insight into water that occurs naturally in confinement, such as that inside cellular vesicles (e.g. lysosomes and endosomes) and could pave the way for improved understanding of their function.

-
- [1] S. Cerveny, F. Mallamace, J. Swenson, M. Vogel, and L. Xu. “Confined Water as Model of Supercooled Water.” *Chem. Rev.*, 116(13):7608–7625 (2016). [doi:10.1021/acs.chemrev.5b00609](https://doi.org/10.1021/acs.chemrev.5b00609).
- [2] R. Biswas and B. Bagchi. “Anomalous water dynamics at surfaces and interfaces: synergistic effects of confinement and surface interactions.” *J. Phys.: Condens. Matter*, 30(1):013001 (2018). [doi:10.1088/1361-648X/aa9b1d](https://doi.org/10.1088/1361-648X/aa9b1d).
- [3] T. Überrück, O. Neudert, K.-D. Kreuer, B. Blümich, J. Granwehr, S. Stapf, and S. Han. “Effect of nitroxide spin probes on the transport properties of Nafion membranes.” *Phys. Chem. Chem. Phys.*, 20(41):26660–26674 (2018). [doi:10.1039/C8CP04607G](https://doi.org/10.1039/C8CP04607G).
- [4] J. M. Franck, R. Kausik, and S. Han. “Overhauser dynamic nuclear polarization-enhanced NMR relaxometry.” *Microporous and Mesoporous Materials*, 178:113–118 (2013). [doi:10.1016/j.micromeso.2013.04.019](https://doi.org/10.1016/j.micromeso.2013.04.019).
- [5] K. G. Valentine, G. Mathies, S. Bédard, N. V. Nucci, I. Dodevski, M. A. Stetz, T. V. Can, R. G. Griffin, and A. J. Wand. “Reverse Micelles As a Platform for Dynamic Nuclear Polarization in Solution NMR of Proteins.” *J. Am. Chem. Soc.*, 136(7):2800–2807 (2014). [doi:10.1021/ja4107176](https://doi.org/10.1021/ja4107176).
- [6] H.-S. Tan, I. R. Piletic, R. E. Riter, N. E. Levinger, and M. D. Fayer. “Dynamics of Water Confined on a Nanometer Length Scale in Reverse Micelles: Ultrafast Infrared Vibrational Echo Spectroscopy.” *Phys. Rev. Lett.*, 94(5):057405 (2005). [doi:10.1103/PhysRevLett.94.057405](https://doi.org/10.1103/PhysRevLett.94.057405).
- [7] I. R. Piletic, D. E. Moilanen, D. B. Spry, N. E. Levinger, and M. D. Fayer. “Testing the Core/Shell Model of Nanoconfined Water in Reverse Micelles Using Linear and Nonlinear IR Spectroscopy.” *J. Phys. Chem. A*, 110(15):4985–4999 (2006). [doi:10.1021/jp061065c](https://doi.org/10.1021/jp061065c).
- [8] M. R. Harpham, B. M. Ladanyi, N. E. Levinger, and K. W. Herwig. “Water motion in reverse micelles studied by quasielastic neutron scattering and molecular dynamics simulations.” *J. Chem. Phys.*, 121(16):7855 (2004). [doi:10.1063/1.1792592](https://doi.org/10.1063/1.1792592).
- [9] A. A. Beaton, A. Guinness, and J. M. Franck. “Rapidly screening the correlation between the rotational mobility and the hydrogen bonding strength of confined water.” *preprint (arxiv forthcoming)* (2023).
- [10] G. M. Clore and J. Iwahara. “Theory, Practice, and Applications of Paramagnetic Relaxation Enhancement for the Characterization of Transient Low-Population States of Biological Macromolecules and Their Complexes.” *Chemical Reviews*, 109(9):4108–4139 (2009). [doi:10.1021/cr900033p](https://doi.org/10.1021/cr900033p).
- [11] J. M. Franck, M. Sokolovski, N. Kessler, E. Matalon, M. Gordon-Grossman, S.-i. Han, D. Goldfarb, and A. Horovitz. “Probing Water Density and Dynamics in the Chaperonin GroEL Cavity.” *Journal of the American Chemical Society*, 136(26):9396–9403 (2014). [doi:10.1021/ja503501x](https://doi.org/10.1021/ja503501x).
- [12] J. M. Franck and S. Han. “Overhauser Dynamic Nuclear Polarization for the Study of Hydration Dynamics, Explained.” In A. J. Wand, editor, “Biological NMR Part B,” volume 615 of *Methods in Enzymology*, pages 131–

175. Academic Press (2019).
- [13] R. Barnes, S. Sun, Y. Fichou, F. W. Dahlquist, M. Heyden, and S. Han. “Spatially Heterogeneous Surface Water Diffusivity around Structured Protein Surfaces at Equilibrium.” *Journal of the American Chemical Society*, 139(49):17890–17901 (2017). [doi:10.1021/jacs.7b08606](https://doi.org/10.1021/jacs.7b08606).
- [14] N. Bloembergen, E. M. Purcell, and R. V. Pound. “Relaxation Effects in Nuclear Magnetic Resonance Absorption.” *Physical Review*, 73(7):679–712 (1948). [doi:10.1103/PhysRev.73.679](https://doi.org/10.1103/PhysRev.73.679).
- [15] I. Solomon. “Relaxation Processes in a System of Two Spins.” *Physical Review*, 99(2):559–565 (1955). [doi:10.1103/PhysRev.99.559](https://doi.org/10.1103/PhysRev.99.559).
- [16] H. H. Mantsch, H. Saitô, and I. C. P. Smith. “Deuterium magnetic resonance, applications in chemistry, physics and biology.” *Prog. Nucl. Magn. Reson. Spectrosc.*, 11(4):211–272 (1977). [doi:10.1016/0079-6565\(77\)80010-1](https://doi.org/10.1016/0079-6565(77)80010-1).
- [17] J. Winsberg, C. Stolze, A. Schwenke, S. Muench, M. D. Hager, and U. S. Schubert. “Aqueous 2,2,6,6-Tetramethylpiperidine-N-oxyl Catholytes for a High-Capacity and High Current Density Oxygen-Insensitive Hybrid-Flow Battery.” *ACS Energy Letters*, 2(2):411–416 (2017). [doi:10.1021/acsenergylett.6b00655](https://doi.org/10.1021/acsenergylett.6b00655).
- [18] E. E. Fenn, D. B. Wong, and M. D. Fayer. “Water dynamics in small reverse micelles in two solvents: Two-dimensional infrared vibrational echoes with two-dimensional background subtraction.” *J. Chem. Phys.*, 134(5):054512 (2011). [doi:10.1063/1.3532542](https://doi.org/10.1063/1.3532542).
- [19] G. Haering, P. L. Luisi, and H. Hauser. “Characterization by electron spin resonance of reversed micelles consisting of the ternary system AOT-isoctane-water.” *The Journal of Physical Chemistry*, 92(12):3574–3581 (1988). [doi:10.1021/j100323a050](https://doi.org/10.1021/j100323a050).
- [20] H. Hauser, G. Haering, A. Pande, and P. L. Luisi. “Interaction of water with sodium bis(2-ethyl-1-hexyl) sulfosuccinate in reversed micelles.” *The Journal of Physical Chemistry*, 93(23):7869–7876 (1989). [doi:10.1021/j100360a029](https://doi.org/10.1021/j100360a029).
- [21] D. E. Moilanen, E. E. Fenn, D. Wong, and M. D. Fayer. “Water dynamics in large and small reverse micelles: From two ensembles to collective behavior.” *The Journal of Chemical Physics*, 131(1) (2009). PMID: 19586114. [doi:10.1063/1.3159779](https://doi.org/10.1063/1.3159779).
- [22] G. Schirò, Y. Fichou, F.-X. Gallat, K. Wood, F. Gabel, M. Moulin, M. Härtlein, M. Heyden, J.-P. Colletier, A. Orecchini, A. Paciaroni, J. Wuttke, D. J. Tobias, and M. Weik. “Translational diffusion of hydration water correlates with functional motions in folded and intrinsically disordered proteins.” *Nature Communications*, 6(1):6490 (2015). [doi:10.1038/ncomms7490](https://doi.org/10.1038/ncomms7490).